

# Role of two-electron processes in the excitation-ionization of lithium atoms by fast ion impact

T. Kirchner\* and N. Khazai

*Department of Physics and Astronomy,  
York University, Toronto, Ontario, Canada, M3J 1P3*

L. Gulyás

*Institute for Nuclear Research, Hungarian Academy of Sciences (ATOMKI),  
P.O. Box 51, H-4001 Debrecen, Hungary*

(Dated: July 22, 2021)

## Abstract

We study excitation and ionization in the 1.5 MeV/amu  $O^{8+}$ -Li collision system, which was the subject of a recent reaction-microscope-type experiment [Fischer *et al.*, Phys. Rev. Lett. **109**, 113202 (2012)]. Starting from an independent-electron model based on determinantal wave functions and using single-electron basis generator method and continuum distorted-wave with eikonal initial-state calculations we show that pure single ionization of a lithium  $K$ -shell electron is too weak a process to explain the measured single differential cross section. Rather, our analysis suggests that two-electron excitation-ionization processes occur and have to be taken into account when comparing with the data. Good agreement is obtained only if we replace the independent-electron calculation by an independent-event model for one of the excitation-ionization processes and also take a shake-off process into account.

PACS numbers: 34.50.Fa

---

\* tomk@yorku.ca

## I. INTRODUCTION

The investigation and differentiation of single and multiple electron processes has been a topic of considerable interest in atomic collision physics over many years. For one thing, studies in this area shed light on questions relevant for applied research, e.g., in radiation therapy, where the damage induced by swift ions is different in single- and multiple-ionization events [1]. Multiple ionization of, e.g., water molecules results in fragmentation practically with certainty, while there is a high chance that the  $\text{H}_2\text{O}^+$  ion created after single-electron removal stays intact [2].

Much of the experimental and theoretical activity in the investigation of single and multiple processes is, however, fueled by the fundamental interest in the few-body quantum dynamics at play. The seemingly simplest situation that can occur in an ion-atom collision corresponds to single-electron removal, in which one target electron is either captured by the (bare) projectile or promoted to a continuum state. However, single-electron removal is not necessarily a pure one-electron process: Another target electron may participate in the dynamics and end up in an excited state after the collision. In the case of capture, these so-called transfer plus target-excitation (TTE) events have been identified in cold target recoil ion momentum spectroscopy (COLTRIMS) and reaction microscope (ReMi) experiments, which give access to the  $Q$ -value of a given reaction, i.e., the electronic energy loss or gain [3–5]. Excitation-ionization (EI) was measured some time ago at very high projectile energy using (Auger-) electron spectroscopy [6].

If the target atom is helium, which has often been the case in COLTRIMS and ReMi experiments, TTE and EI are true two-electron processes. A somewhat different situation arises if more than one target shell is occupied before the collision. In this case, the single capture or single ionization of an inner-shell electron leaves the target ion behind in an excited state. In a naive independent-particle picture a two-electron process, in which an outer-shell electron is removed and an inner-shell electron is promoted to the state just vacated, has the same outcome. This type of two-electron TTE or EI in principle becomes distinguishable from pure single inner-shell electron removal if the inner-shell electron is promoted to a target state that was vacant before the collision[7]. In practice, however, the resolution achievable in  $Q$ -value measurements may make it difficult to separate these two-electron processes from pure one-electron removal. Theoretical calculations are then

required for a full understanding of the situation.

A recent joint experimental-theoretical work on 1.5 MeV/amu  $O^{8+}$  collisions from lithium atoms was concerned with this problem [8]. The experiments were performed with the newly-developed 'MOTReMi' apparatus, which combines a magneto-optical trap (MOT) to cool the lithium atoms with a ReMi to measure the reaction products. The recorded  $Q$ -value spectra for single ionization exhibit two distinct peaks, which can be associated with the ejection of the  $2s$  valence electron and the ejection of an inner  $K$ -shell electron, respectively. A continuum distorted-wave with eikonal initial-state (CDW-EIS) calculation for  $Li(2s)$  ionization was found to be in reasonable agreement with the measured electron-energy single differential cross section (SDCS) corresponding to the first peak, but a CDW-EIS calculation for  $Li(1s)$  ionization differed markedly from the data in the other channel. It was concluded that two-electron EI, which was not taken into account in the calculation, is needed to explain the measurement.

In this paper, we provide a theoretical analysis of the  $O^{8+}$ -Li collision system based on the independent-electron (IEL) model to scrutinize this interpretation. The IEL model is discussed in Sec. II. In Sec. III, we present IEL SDCSs for various pure ionization and EI processes and compare them with the experimental data. Extensions of the IEL model, among them an independent-event (IEV) model for one EI process, are considered to account for the quite substantial discrepancies. A summarizing discussion is provided in Sec. IV. Atomic units characterized by  $\hbar = m_e = e = 4\pi\epsilon_0 = 1$  are used unless otherwise stated.

## II. INDEPENDENT-ELECTRON TREATMENT OF PURE SINGLE IONIZATION AND EXCITATION-IONIZATION

Within the semiclassical approximation (SCA) the  $O^{8+}$ -Li collision system is described by a time-dependent Schrödinger equation (TDSE) for the electronic Hamiltonian

$$\hat{H}_e(t) = \sum_{i=1}^N [\hat{T}_i + \hat{V}_i^{en}(t)] + \sum_{i<j}^N \hat{W}_{ij}, \quad (1)$$

which consists of single-electron kinetic energy operators  $\hat{T}_i$ , electron-nucleus interactions  $\hat{V}_i^{en}$  (which depend on time due to the SCA assumption of classically moving nuclei), and the electron-electron Coulomb interactions  $\hat{W}_{ij}$ . To the best of our knowledge an explicit solution of this correlated  $N=3$ -electron problem has not been attempted yet.

The IEL model consists in replacing the Hamiltonian (1) by a one-body operator

$$\hat{H}_e(t) \rightarrow \sum_{i=1}^N \hat{h}_i(t) \quad (2)$$

such that the TDSE separates into a set of single-particle equations for the three electrons. We assume the single-particle Hamiltonian to be of the form

$$\hat{h}(t) = -\frac{1}{2}\Delta + V_{\text{Li}}(|\mathbf{r}_t|) - \frac{Z_P}{|\mathbf{r}_p|}, \quad (3)$$

where  $Z_P$  is the charge number of the bare projectile ion, and  $\mathbf{r}_t$  and  $\mathbf{r}_p$  are the position vectors of the electron with respect to the target and the projectile center, respectively. They are related according to  $\mathbf{r}_p = \mathbf{r}_t - \mathbf{R}(t)$  with  $\mathbf{R}(t)$  being the classical straight-line trajectory of the projectile relative to the target center. We note that the Laplace operator in Eq. (3) is taken with respect to the center-of-mass reference frame. The effective potential  $V_{\text{Li}}$  represents the interactions in the  $(1s^2 2s)$  ground-state configuration of the lithium atom. It is obtained from the exchange-only version of the optimized potential method (OPM) of density functional theory [9], i.e., it includes electron-nucleus Coulomb interactions, screening, and exchange terms exactly and exhibits the correct asymptotic  $-1/r_t$  behavior, but it neglects electron correlations.

We have solved the single-particle equations for the Hamiltonian (3) and the initially occupied  $\text{Li}(1s)$  and  $\text{Li}(2s)$  orbitals using the two-center basis generator method (TC-BGM) with a basis that consists of the  $1s - 4f$  target states, the  $1s - 4f$  (hydrogenlike) projectile states, as well as 71 BGM pseudo states to account for ionization [10]. All basis states are endowed with electron translation factors to ensure Galilean invariance. Results for the total excitation ( $p_{1s(2s)}^{\text{exc}}$ ), capture ( $p_{1s(2s)}^{\text{cap}}$ ) and ionization ( $p_{1s(2s)}^{\text{ion}}$ ) probabilities are shown in Fig. 1 as functions of the impact parameter  $b$ . The probabilities are calculated as follows:

$$p_{1s \rightarrow f_k} = |\langle f_k | \psi_{1s}(t_f) \rangle|^2 \quad (4)$$

$$p_{2s \rightarrow f_k} = |\langle f_k | \psi_{2s}(t_f) \rangle|^2 \quad (5)$$

$$p_{1s}^{\text{exc}} = \sum_{f_k \in T, f_k \neq 1s} p_{1s \rightarrow f_k} \quad (6)$$

$$p_{2s}^{\text{exc}} = \sum_{f_k \in T, f_k \neq \{1s, 2s\}} p_{2s \rightarrow f_k} \quad (7)$$

$$p_{1s}^{\text{cap}} = \sum_{f_k \in P} p_{1s \rightarrow f_k} \quad (8)$$

$$p_{2s}^{\text{cap}} = \sum_{f_k \in P} p_{2s \rightarrow f_k} \quad (9)$$

$$p_{1s}^{\text{ion}} = 1 - \sum_{f_k \in T} p_{1s \rightarrow f_k} - \sum_{f_k \in P} p_{1s \rightarrow f_k} \quad (10)$$

$$p_{2s}^{\text{ion}} = 1 - \sum_{f_k \in T} p_{2s \rightarrow f_k} - \sum_{f_k \in P} p_{2s \rightarrow f_k}, \quad (11)$$

where  $|\psi_{1s(2s)}(t_f)\rangle$  denote the solutions of the single-particle equations corresponding to the  $1s(2s)$  initial states and propagated to a sufficiently large final time  $t_f$  after the collision, and  $|f_k\rangle \in T(P)$  are final target (projectile) states. Note that in Eqs. (10) and (11) we use the unitarity of the TC-BGM solutions of the single-particle equations.

As expected at a projectile energy as high as 1.5 MeV/amu, capture is very weak except for the  $1s$  initial state in close collisions. It will be neglected in the following, i.e., we will identify electron removal from the lithium atom with ionization into the continuum. We further observe in Fig. 1 that ionization strongly dominates for the case of the  $1s$  initial state, while for the  $\text{Li}(2s)$  initial state excitation takes over in distant collisions. The details of our calculations show that excitation to  $2p$  is the strongest channel. We also include in Fig. 1 ionization probabilities obtained from a CDW-EIS calculation for the Hamiltonian (3) [11, 12]. They are in very good agreement with the TC-BGM results for the case of the  $1s$  initial state, and still in acceptable agreement for  $2s$ —keeping in mind that the CDW-EIS method is perturbative in nature and the perturbation parameter  $\eta = Z_P/v$  is close to one ( $\eta = 1.03$  for the projectile speed  $v = 7.75$  a.u.).

In order to make contact with the experiment [8] and take EI processes into account, we have to reinstate many-body aspects of the collision system. Consistent with the IEL model this is done by assembling the solutions of the single-particle equations in the form of a

Slater determinant. If the three-electron final states are also taken to be Slater determinants, the transition probabilities of interest can be obtained without further approximation from combinations of determinants constructed from one-particle density matrix elements [13]

$$\langle f_k | \hat{\gamma}^1(t_f) | f_l \rangle = \sum_{i=1}^N \langle f_k | \psi_i(t_f) \rangle \langle \psi_i(t_f) | f_l \rangle. \quad (12)$$

In this work, we are interested in processes, in which exactly one vacancy is created in the lithium atom. They correspond to probabilities for finding two bound single-particle target states, say  $|f_1\rangle$  and  $|f_2\rangle$ , occupied and all the others vacant, and can be calculated according to [13]

$$P_{f_1 f_2}^{\sum_k \bar{f}_k} \equiv P_{f_1 f_2} - \sum_{f_k \in T} P_{f_1 f_2 f_k}. \quad (13)$$

In the expression on the right hand side of Eq. (13)  $P_{f_1 f_2}$  denotes the *inclusive* probability for finding two electrons in the subconfiguration  $|f_1 f_2\rangle$  while nothing is known about the final state of the third electron. As shown in Ref. [13] this inclusive probability is given as the determinant constructed from the  $2 \times 2$  density matrix corresponding to  $|f_1 f_2\rangle$ .  $P_{f_1 f_2 f_k}$  is the *exclusive* probability to find the three electrons in the completely specified configuration  $|f_1 f_2 f_k\rangle$  and is given as the determinant of the  $3 \times 3$  density matrix corresponding to  $|f_1 f_2 f_k\rangle$ . Since the sum in Eq. (13) runs over all bound target states the difference of both terms corresponds to the statement that one of the electrons has been removed from the lithium atom.

For the explicit evaluation of Eq. (13) we have to take the spin projections ( $\uparrow, \downarrow$ ) of the electrons into account and consider spin orbitals that we denote, e.g., by writing  $|f_k \uparrow\rangle$ . Since the Hamiltonian (3) is spin independent we have  $\langle f_k \uparrow | \psi_i \uparrow \rangle = \langle f_k \downarrow | \psi_i \downarrow \rangle = \langle f_k | \psi_i \rangle$  and  $\langle f_k \uparrow | \psi_i \downarrow \rangle = \langle f_k \downarrow | \psi_i \uparrow \rangle = 0$ . We choose the initial state of the lithium atom to be a Slater determinant built from the  $(1s\uparrow 1s\downarrow 2s\uparrow)$  spin orbitals.

With these preparations we are ready to consider the probabilities that correspond to the experimentally distinguishable processes [8]:

- (i)  $2s$  vacancy production  $P_{2s}^{\text{vac}}$ , in which the  $\text{Li}^+$  ion is found in its  $(1s^2)$  ground state:

$$P_{2s}^{\text{vac}} = P_{1s\uparrow 1s\downarrow}^{\sum_k \bar{f}_k \uparrow}, \quad (14)$$

- (ii)  $1s$  vacancy production  $P_{1s}^{\text{vac}}$ , in which the  $\text{Li}^+$  ion is left in the excited configuration

( $1snl$ ) with  $n \geq 2$ :

$$P_{1s}^{\text{vac}} = \sum_{f_i \in T, f_i \neq 1s} (P_{1s \uparrow f_i \uparrow}^{\sum_k \bar{f}_k \downarrow} + P_{1s \uparrow f_i \downarrow}^{\sum_k \bar{f}_k \uparrow} + P_{1s \downarrow f_i \uparrow}^{\sum_k \bar{f}_k \uparrow}). \quad (15)$$

All terms on the right hand sides of Eqs. (14) and (15) can be computed using the prescription (13). It is instructive to work out the determinants analytically. With the definitions (4) to (11) and

$$p_{1s}^{\text{elast}} = p_{1s \rightarrow 1s} \quad (16)$$

$$p_{2s}^{\text{elast}} = p_{2s \rightarrow 2s} \quad (17)$$

one obtains

$$P_{2s}^{\text{vac}} = P_{2s}^{\text{excl}} + P_{2s}^{\text{ex}} + \Delta P_{2s}^{\text{anti}} \quad (18)$$

$$P_{1s}^{\text{vac}} = P_{1s}^{\text{excl}} + P_{EI1} + P_{EI2} + P_{1s}^{\text{ex}} + \Delta P_{1s}^{\text{anti}} \quad (19)$$

with

$$P_{2s}^{\text{excl}} = (p_{1s}^{\text{elast}})^2 p_{2s}^{\text{ion}} \quad (20)$$

$$P_{2s}^{\text{ex}} = p_{1s}^{\text{elast}} p_{1s}^{\text{ion}} p_{2s \rightarrow 1s} \quad (21)$$

$$P_{1s}^{\text{excl}} = 2p_{1s}^{\text{elast}} p_{1s}^{\text{ion}} p_{2s}^{\text{elast}} \quad (22)$$

$$P_{EI1} = 2p_{1s}^{\text{elast}} p_{1s}^{\text{ion}} p_{2s}^{\text{exc}} \quad (23)$$

$$P_{EI2} = 2p_{1s}^{\text{elast}} p_{1s}^{\text{exc}} p_{2s}^{\text{ion}} \quad (24)$$

$$P_{1s}^{\text{ex}} = 2p_{1s}^{\text{exc}} p_{1s}^{\text{ion}} p_{2s \rightarrow 1s} \quad (25)$$

and correction terms  $\Delta P_{1s}^{\text{anti}}$  and  $\Delta P_{2s}^{\text{anti}}$  stemming from off-diagonal elements of the density matrix that reflect the antisymmetry of the three-electron wave functions. These terms as well as a few details regarding the derivation of Eqs. (18) and (19) are given in the Appendix.

Equations (20) to (25) have straightforward interpretations and can also be obtained from a simple multinomial analysis of the three-electron problem that is based on associating each electron with a single-particle probability. Expressions (20) and (22) correspond to exclusive ionization events, in which the non-ionized electrons remain bound in their initial states. The probabilities (23) and (24) correspond to two-electron EI processes, in which one  $K$ -shell electron does not change its state, while the other two electrons are either excited or ionized. Finally, Eqs. (21) and (25) describe exchange processes which arise as a consequence of

the indistinguishability of the electrons. In practice, these exchange terms as well as the correction terms  $\Delta P_{1s}^{\text{anti}}$  and  $\Delta P_{2s}^{\text{anti}}$  are negligible.

This is demonstrated in Figs. 2 and 3. Figure 2 displays the  $b$ -weighted probability for  $2s$  vacancy production according to Eq. (14). Differences to exclusive  $2s$  ionization according to Eq. (20) are too small to be visible mainly because the exchange amplitude for a transition from the  $2s$  to the  $1s$  state in the correction terms is very small. We have also included  $p_{2s}^{\text{ion}}$  in Fig. 2. This probability is interpreted as the single-ionization probability in a one-active-electron (OAE) model in which the two  $K$ -shell electrons are assumed to be frozen throughout the collision. Obviously, the OAE result differs from the other curves only at relatively small  $b$ , where the  $1s$  electrons do undergo transitions with non-negligible probabilities.

In Fig. 3 we show  $b$ -weighted probabilities for processes that result in the creation of one  $K$ -shell vacancy.  $P_{EI1}$  [Eq. (23)] is almost as strong as  $P_{1s}^{\text{excl}}$  [Eq. (22)], whereas  $P_{EI2}$  [Eq. (24)], which involves the excitation of a  $K$ -shell electron, is considerably weaker. The sum of these three probabilities is in almost perfect agreement with the full result for  $1s$  vacancy production according to Eq. (15)—demonstrating that also for  $1s$  ionization the exchange and antisymmetry correction terms in Eq. (19) can be neglected.

In many calculations for helium targets the quantity  $2p_{1s}^{\text{ion}}$  was used to calculate ionization cross sections (see, e.g., Ref. [14, 15]). This procedure again corresponds to an OAE model, in which the factor of two arises since one does not know which of the two  $K$ -shell electrons is active and which is passive. We have included a  $2p_{1s}^{\text{ion}}$  curve in Fig. 3. It is seen to be much larger than the other probabilities, which indicates that the assumption of just one active  $K$ -shell electron is not realistic for the 1.5 MeV  $\text{O}^{8+}$ -Li collision system. The main reason for this is that it is very unlikely for the initial  $2s$  electron not to undergo a transition in a relatively close collision. Put another way, if the assumption of two passive electrons is unrealistic, the quantity  $2p_{1s}^{\text{ion}}$  is contaminated by multielectron processes.

### III. DIFFERENTIAL CROSS SECTION RESULTS AND EXTENSIONS OF THE IEL MODEL

Having analyzed the relative strengths of various ionization processes within the IEL model we now turn to the SDCSs for the two reaction channels discussed in Ref. [8]. Ideally,



we would calculate them on the basis of Eqs. (14) and (15) and the TC-BGM single-particle solutions. However, this is not possible, since it is difficult to extract electron-emission-energy ( $E_e$ ) differential information from the population of the BGM pseudo states. Instead, we use the CDW-EIS method to calculate single-particle ionization probabilities  $p_i^{\text{ion}}(b, E_e)$  for  $i = 1s, 2s$  and combine them with the  $b$ -dependent TC-BGM probabilities for excitations and elastic transitions according to the simplified Eqs. (20), (22), (23), and (24). The resulting  $b$  and  $E_e$  dependent probabilities are integrated over the impact parameter in order to obtain the  $E_e$ -differential SDCSs. Given that (i) the exchange and antisymmetry correction terms in Eqs. (18) and (19) were shown to be small, and (ii) the CDW-EIS total ionization probabilities  $p_i^{\text{ion}}(b)$  were shown to be close to their TC-BGM counterparts this procedure is unlikely to produce errors in addition to those stemming from the limitations of the IEL model.

Results are shown in Fig. 4 in comparison with the experimental data of Ref. [8]. For the  $2s$  channel the OAE and exclusive ionization SDCSs are very similar (cf. Fig. 2) and in reasonable agreement with the data, which were deemed low at energies  $E_e > 20$  eV due to acceptance limitations of the spectrometer [8]. We note that the present results are in very good agreement with the CDW-EIS calculations shown in Fig. 2(b) of Ref. [8], which we did not include in our figure for the sake of clarity.

For the  $1s$  channel the situation is more involved. Our OAE result agrees well with the CDW-EIS calculation reported in Ref. [8] (not shown), but it differs in both magnitude and shape from the experimental data. As mentioned earlier, the OAE cross section is contaminated by multielectron processes, particularly by multiple ionization, which is excluded in the measured coincidences of electrons and singly-charged ions. Hence, this quantity is not very useful for the analysis of the experimental data. On the other hand, exclusive  $1s$  ionization is much smaller than the measurements at all electron energies. The same is true for the EI process described by Eq. (23), which consists of  $1s$  ionization and  $2s$  excitation. Similarly to exclusive  $1s$  ionization this EI process reflects the energy dependence of the OAE  $1s$  ionization curve, which can be inferred from Eqs. (22) and (23).

Likewise, the other EI process [Eq. (24)] which involves  $2s$  ionization and  $1s$  excitation reflects the energy dependence of the  $2s$  ionization curve. If one adds it to exclusive  $1s$  ionization and  $1s$  ionization with  $2s$  excitation to calculate the total IEL SDCS for  $1s$ -vacancy production one obtains a curve whose shape has some similarity with the energy

dependence of the experimental data, but lies significantly below them except at the highest electron energies. We thus have to conclude that the IEL model is not sufficient to explain the measurements.

In an attempt to understand the discrepancy without embarking on a full solution of the correlated three-electron problem we have considered the following scenarios. First, one may argue that for the EI process corresponding to Eq. (24) a sequential IEV picture of the collision dynamics is more realistic than the IEL model. In such a scenario the outer ( $2s$ ) electron is removed first with the result that the inner ( $1s$ ) electrons rearrange before one of them is promoted to an excited state of the  $\text{Li}^+$  ion. Accordingly, we also considered a Hamiltonian in which the OPM potential  $V_{\text{Li}}$  is replaced by the OPM potential  $V_{\text{Li}^+}$  for the ( $1s^2$ ) configuration which decays like  $-2/r_t$  asymptotically. The  $1s$ -excitation with  $2s$ -ionization SDCS in the IEV model was then calculated according to

$$\left(\frac{d\sigma}{dE_e}\right)_{\text{IEV}} = 2 \int d^2b p_{1s^+}^{\text{elast}}(b) p_{1s^+}^{\text{exc}}(b) p_{2s}^{\text{ion}}(b, E_e), \quad (26)$$

where  $p_{1s^+}^{\text{elast}}(b)$  and  $p_{1s^+}^{\text{exc}}(b)$  denote single-particle elastic and excitation probabilities obtained from TC-BGM collision calculations for  $\text{O}^{8+}\text{-Li}^+$ , and  $p_{2s}^{\text{ion}}(b, E_e)$  is the electron-energy differential CDW-EIS ionization probability for  $\text{O}^{8+}\text{-Li}$  that we also used in the IEL calculations. We note that we did not consider the IEV counterpart of the EI process (23), in which a  $K$ -shell electron is removed and the  $2s$  electron excited, since it does not seem plausible to assume that the wave function of the outer  $2s$  electron adjusts to an ionic ( $1s2s$ ) configuration after inner-shell ionization. Besides, we know from the analysis presented above that such an IEV probability would result in the same  $E_e$ -dependence as OAE  $1s$  ionization, which is at odds with the measured data.

Secondly, our TC-BGM basis only includes target states up to principal quantum number  $n = 4$ . It is impossible to push the calculation further without severely restricting the representation of the continuum. In order to estimate the contribution from higher excitations we have assumed that they scale like  $1/n^3$  which allows for extrapolating them to  $n \rightarrow \infty$  [16].

Finally, we have estimated the contribution from a correlated two-electron process, in which a  $1s$  electron is excited and the  $2s$  electron is emitted due to shake-off. We have calculated the ( $E_e$ -differential) shake probability by projecting the  $\text{Li}(2s)$  state onto continuum states of the single-center Hamiltonian

$$\hat{h}_{\text{shake}} = -\frac{1}{2}\Delta_{r_t} - \frac{Z_T}{r_t} + \frac{1}{r_t}[1 - (1 + Z_T r_t)e^{-2Z_T r_t}]. \quad (27)$$

For  $Z_T = 3$  the total potential of this Hamiltonian corresponds to the sum of the Coulomb potential of the lithium nucleus and an electrostatic potential due to the presence of one hydrogenlike  $1s$  electron, i.e., the effects due to the presence of the excited electron and the repulsion between the  $1s$  and  $2s$  electrons are neglected. We have repeated the shake-off calculation with continuum states of the  $\text{Li}^+$  Hamiltonian used in the IEV calculation and have found very similar results indicating that these simplifications are of minor importance.

Figure 5 displays the results of these extensions. The IEV SDCS (26) gives the strongest contribution. The correction due to the  $n \rightarrow \infty$  extrapolation amounts to about 20% and is included in the cross section curve shown. The strongest partial channels are those corresponding to the dipole-allowed excitations into  $2p$  ( $\sim 44\%$ ) and  $3p$  ( $\sim 13\%$ ). Interestingly, the IEV SDCS is much stronger than its IEL counterpart for the process (24) shown in Fig. 4. This mirrors the fact that the single-particle excitation probabilities for the lithium ion ( $p_{1s+}^{\text{exc}}$ ) are larger than those for the atom ( $p_{1s}^{\text{exc}}$ ), which can be understood by inspecting the orbital densities of the single-particle states involved. As shown in Fig. 6 the  $\text{Li}^+(1s)$  and  $\text{Li}(1s)$  densities are practically indistinguishable on a linear plot. They only differ in their asymptotic decays which are determined by the energy eigenvalues (indicated as horizontal lines in Fig. 6). By contrast, the excited states are markedly different with those of  $\text{Li}^+$  being more compact than those of  $\text{Li}$  and thus easier accessible for an initial  $K$ -shell electron. Figure 6 shows that in the case of the neutral lithium atom the  $1s$  and  $2p$  states have only very little spatial overlap. These observations favor the IEV picture, because the ionic excited states are more realistic final states for EI than the neutral atom states. Figure 6 also displays the  $\text{Li}$  and  $\text{Li}^+$  OPM potentials. The shoulder in the neutral atom potential is a reflection of the shell structure.

Coming back to Fig. 5, we observe that the  $1s$  ionization with  $2s$  excitation SDCS corresponding to Eq. (23) increases by a little less than 20% when the contribution from excitations to  $n \geq 5$  is included, and becomes very similar to the exclusive  $1s$  ionization curve (which is repeated in Fig. 5). Again the  $2p$  excitation channel is the strongest one, contributing almost half of the cross section. The shake-off SDCS, obtained by replacing  $p_{2s}^{\text{ion}}$  in Eq. (24) by the shake probability, applying the  $n \rightarrow \infty$  correction to  $p_{1s}^{\text{exc}}$  and integrating over the impact parameter, falls off steeply with increasing electron energy, but it does give a non-negligible contribution at low  $E_e$ . When added to the three other contributions shown in Fig. 5 we obtain the thick full curve. The agreement with the measurements is not perfect,

but it is very good down to  $E_e \approx 2$  eV.

#### IV. SUMMARY

In this work, we have used the independent-electron model to analyze the contributions from single ionization with and without additional target excitation to the recent MOTReMi SDCS measurements for 1.5 MeV/amu  $O^{8+}$ -Li collisions. Our results, obtained by combining TC-BGM and CDW-EIS single-particle probabilities, largely confirm what was speculated in Ref. [8]: Two-electron excitation-ionization processes occur and must be taken into account when comparing with the measurements for the  $1s$  channel. However, the independent-electron model is not sufficient to explain the data. Rather, we had to replace it by an independent-event calculation for one of the EI processes, i.e., we had to take relaxation effects into account, and we also had to include a shake-off process to obtain good agreement with the measurements. Accordingly, we have to conclude that electron correlation effects play some role in this collision system.

It would be of interest to extend the experimental and theoretical studies by varying the collision parameters projectile charge and velocity. This would provide additional insight into the limitations of the independent-electron model and the role of relaxation and shake-off processes. Ultimately, the theoretical challenge consists in carrying out a full three-electron calculation for this collision system.

#### ACKNOWLEDGMENTS

This work was supported by the Natural Sciences and Engineering Research Council of Canada (NSERC) and by the Hungarian Scientific Research Fund (OTKA Grant No. K 109440). We thank Eberhard Engel for making his atomic structure calculations available to us.

#### Appendix

According to Eqs. (13) and (14) the  $2s$  vacancy production  $P_{2s}^{\text{vac}}$  is given as

$$P_{2s}^{\text{vac}} = P_{1s\uparrow 1s\downarrow} - \sum_{f_k \in T} P_{1s\uparrow 1s\downarrow f_k\uparrow}. \quad (\text{A.1})$$

The inclusive probability  $P_{1s\uparrow 1s\downarrow}$  is the determinant of the  $2 \times 2$  density matrix corresponding to the configuration  $(1s \uparrow 1s \downarrow)$ :

$$P_{1s\uparrow 1s\downarrow} = \begin{vmatrix} \langle 1s \uparrow | \hat{\gamma}^1(t_f) | 1s \uparrow \rangle & \langle 1s \uparrow | \hat{\gamma}^1(t_f) | 1s \downarrow \rangle \\ \langle 1s \downarrow | \hat{\gamma}^1(t_f) | 1s \uparrow \rangle & \langle 1s \downarrow | \hat{\gamma}^1(t_f) | 1s \downarrow \rangle \end{vmatrix}, \quad (\text{A.2})$$

where [cf. Eq. (12)]

$$\hat{\gamma}^1(t_f) = |\psi_{1s\uparrow}(t_f)\rangle\langle\psi_{1s\uparrow}(t_f)| + |\psi_{1s\downarrow}(t_f)\rangle\langle\psi_{1s\downarrow}(t_f)| + |\psi_{2s\uparrow}(t_f)\rangle\langle\psi_{2s\uparrow}(t_f)|. \quad (\text{A.3})$$

Inserting (A.3) into (A.2), exploiting spin orthogonality and omitting the time argument for convenience we obtain

$$P_{1s\uparrow 1s\downarrow} = \begin{vmatrix} |\langle 1s | \psi_{1s} \rangle|^2 + |\langle 1s | \psi_{2s} \rangle|^2 & 0 \\ 0 & |\langle 1s | \psi_{1s} \rangle|^2 \end{vmatrix} = (p_{1s}^{\text{elast}})^2 + p_{1s}^{\text{elast}} p_{2s \rightarrow 1s}. \quad (\text{A.4})$$

In the last step we have used the definitions (4), (5), and (16).

The exclusive probability  $P_{1s\uparrow 1s\downarrow f_k\uparrow}$  is the determinant of the  $3 \times 3$  density matrix corresponding to the configuration  $(1s \uparrow 1s \downarrow f_k \uparrow)$ . Using similar arguments as above we can write

$$P_{1s\uparrow 1s\downarrow f_k\uparrow} = \begin{vmatrix} |\langle 1s | \psi_{1s} \rangle|^2 + |\langle 1s | \psi_{2s} \rangle|^2 & 0 & \langle 1s | \psi_{1s} \rangle \langle \psi_{1s} | f_k \rangle + \langle 1s | \psi_{2s} \rangle \langle \psi_{2s} | f_k \rangle \\ 0 & |\langle 1s | \psi_{1s} \rangle|^2 & 0 \\ \langle f_k | \psi_{1s} \rangle \langle \psi_{1s} | 1s \rangle + \langle f_k | \psi_{2s} \rangle \langle \psi_{2s} | 1s \rangle & 0 & |\langle f_k | \psi_{1s} \rangle|^2 + |\langle f_k | \psi_{2s} \rangle|^2 \end{vmatrix} \\ = (p_{1s}^{\text{elast}})^2 p_{2s \rightarrow f_k} + p_{1s}^{\text{elast}} [p_{1s \rightarrow f_k} p_{2s \rightarrow 1s} - (\langle 1s | \psi_{1s} \rangle \langle \psi_{1s} | f_k \rangle \langle f_k | \psi_{2s} \rangle \langle \psi_{2s} | 1s \rangle + c.c.)], \quad (\text{A.5})$$

where *c.c.* denotes the complex conjugate. One easily infers from the last expression of Eq. (A.5) that  $P_{1s\uparrow 1s\downarrow f_k\uparrow} = 0$  for  $|f_k\rangle = |1s\rangle$  as is required by the Pauli principle.

Inserting (A.4) and (A.5) in (A.1) we obtain

$$P_{2s}^{\text{vac}} = (p_{1s}^{\text{elast}})^2 \left( 1 - \sum_{f_k \in T} p_{2s \rightarrow f_k} \right) + p_{1s}^{\text{elast}} p_{2s \rightarrow 1s} \left( 1 - \sum_{f_k \in T} p_{1s \rightarrow f_k} \right) \\ + p_{1s}^{\text{elast}} \sum_{f_k \in T} (\langle 1s | \psi_{1s} \rangle \langle \psi_{1s} | f_k \rangle \langle f_k | \psi_{2s} \rangle \langle \psi_{2s} | 1s \rangle + c.c.). \quad (\text{A.6})$$

In the last step we use the definitions for single-particle ionization (10) and (11) and remember that capture is negligible to obtain Eq. (18) with the abbreviations (20) and (21) and the correction term

$$\Delta P_{2s}^{\text{anti}} = p_{1s}^{\text{elast}} \sum_{f_k \in T} (\langle 1s | \psi_{1s} \rangle \langle \psi_{1s} | f_k \rangle \langle f_k | \psi_{2s} \rangle \langle \psi_{2s} | 1s \rangle + c.c.). \quad (\text{A.7})$$

Equation (19) for the  $1s$  vacancy production  $P_{1s}^{\text{vac}}$  can be derived using similar arguments. The calculation is straightforward but lengthy. One finds for the correction term:

$$\begin{aligned}
\Delta P_{1s}^{\text{anti}} = & -p_{1s}^{\text{ion}} \sum_{f_k \in T, f_k \neq 1s} (\langle 1s | \psi_{1s} \rangle \langle \psi_{1s} | f_k \rangle \langle f_k | \psi_{2s} \rangle \langle \psi_{2s} | 1s \rangle + c.c.) \\
& + p_{1s}^{\text{exc}} \sum_{f_k \in T} (\langle 1s | \psi_{1s} \rangle \langle \psi_{1s} | f_k \rangle \langle f_k | \psi_{2s} \rangle \langle \psi_{2s} | 1s \rangle + c.c.) \\
& + p_{1s}^{\text{elast}} \sum_{f_k \in T} \sum_{f_l \in T, f_l \neq 1s} (\langle f_k | \psi_{1s} \rangle \langle \psi_{1s} | f_l \rangle \langle f_l | \psi_{2s} \rangle \langle \psi_{2s} | f_k \rangle + c.c.). \quad (\text{A.8})
\end{aligned}$$

- 
- [1] B. Gervais, M. Beuve, G. H. Olivera, and M. E. Galassi, *Radiat. Phys. Chem.* **75**, 493 (2006).
- [2] M. Murakami, T. Kirchner, M. Horbatsch, and H. J. Lüdde, *Phys. Rev. A* **85**, 052713 (2012).
- [3] A. Hasan, B. Tooke, M. Zapukhlyak, T. Kirchner, and M. Schulz, *Phys. Rev. A* **74**, 032703 (2006).
- [4] M. S. Schöffler, J. N. Titze, L. P. H. Schmidt, T. Jahnke, O. Jagutzki, H. Schmidt-Böcking, and R. Dörner, *Phys. Rev. A* **80**, 042702 (2009).
- [5] D. L. Guo, X. Ma, S. F. Zhang, X. L. Zhu, W. T. Feng, R. T. Zhang, B. Li, H. P. Liu, S. C. Yan, P. J. Zhang, and Q. Wang, *Phys. Rev. A* **86**, 052707 (2012).
- [6] J. A. Tanis, J.-Y. Chesnel, F. Frémont, D. Hennecart, X. Husson, A. Cassimi, J. P. Grandin, B. Skogvall, B. Sulik, J.-H. Bremer, and N. Stolterfoht, *Phys. Rev. Lett.* **83**, 1131 (1999).
- [7] It is indistinguishable though from another two-electron process that involves inner-shell electron removal and outer-shell electron excitation; see the discussion of Eq. (19) in Sec. II.
- [8] D. Fischer, D. Globig, J. Goullon, M. Grieser, R. Hubele, V. L. B. de Jesus, A. Kelkar, A. LaForge, H. Lindenblatt, D. Misra, B. Najjari, K. Schneider, M. Schulz, M. Sell, and X. Wang, *Phys. Rev. Lett.* **109**, 113202 (2012).
- [9] E. Engel and S. H. Vosko, *Phys. Rev. A* **47**, 2800 (1993).
- [10] M. Zapukhlyak, T. Kirchner, H. J. Lüdde, S. Knoop, R. Morgenstern, and R. Hoekstra, *J. Phys. B* **38**, 2353 (2005).
- [11] D. S. F. Crothers and J. F. McCann, *J. Phys. B* **16**, 3229 (1983).
- [12] P. D. Fainstein, L. Gulyás, and A. Salin, *J. Phys. B* **29**, 1225 (1996).
- [13] H. J. Lüdde and R. M. Dreizler, *J. Phys. B* **18**, 107 (1985).
- [14] L. Gulyás, A. Igarashi, P. D. Fainstein, and T. Kirchner, *J. Phys. B* **41**, 025202 (2008).

- [15] L. Gulyás, A. Igarashi, and T. Kirchner, *J. Phys. B* **45**, 085205 (2012).
- [16] D. Röhrbein, T. Kirchner, and S. Fritzsche, *Phys. Rev. A* **81**, 042701 (2010).

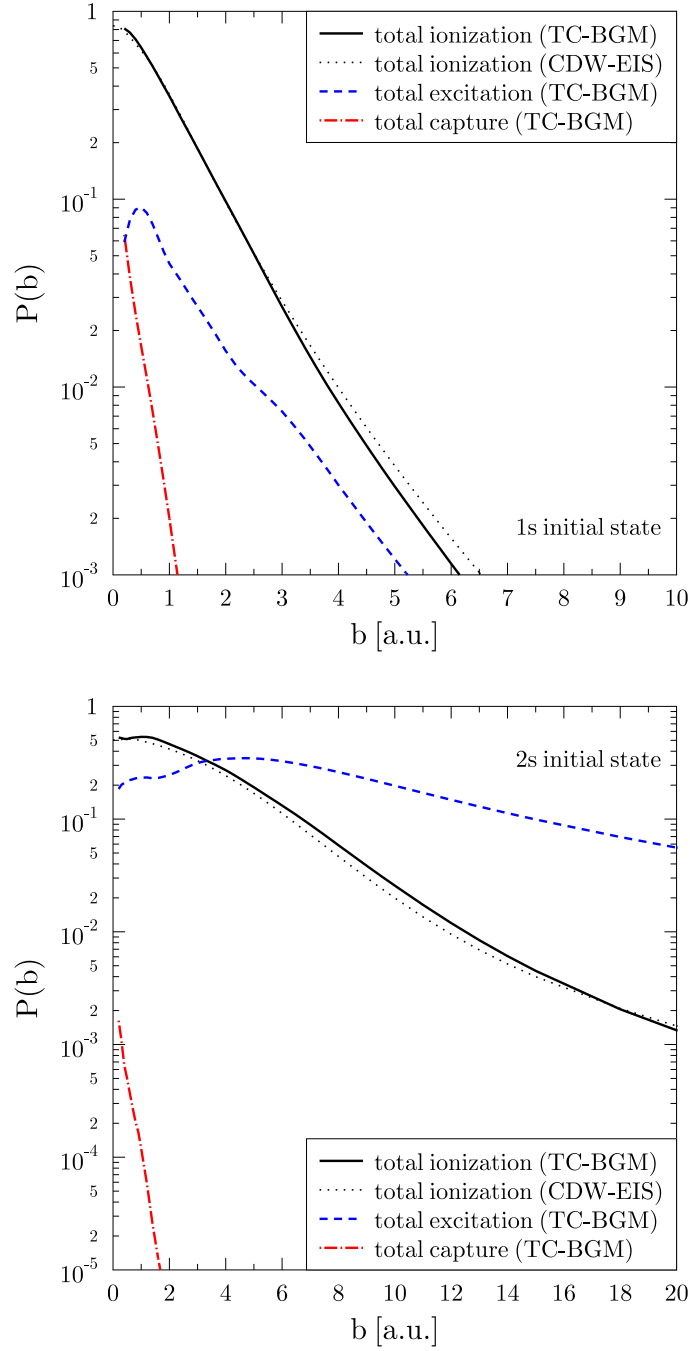


FIG. 1. (Color online) Total excitation, capture, and ionization probabilities according to Eqs. (6) to (11) for 1.5 MeV/amu  $O^{8+}$ -Li collisions obtained from TC-BGM calculations for Li(1s) (upper panel) and Li(2s) (lower panel) initial states. CDW-EIS ionization probabilities are displayed in addition as (black) dotted curves.



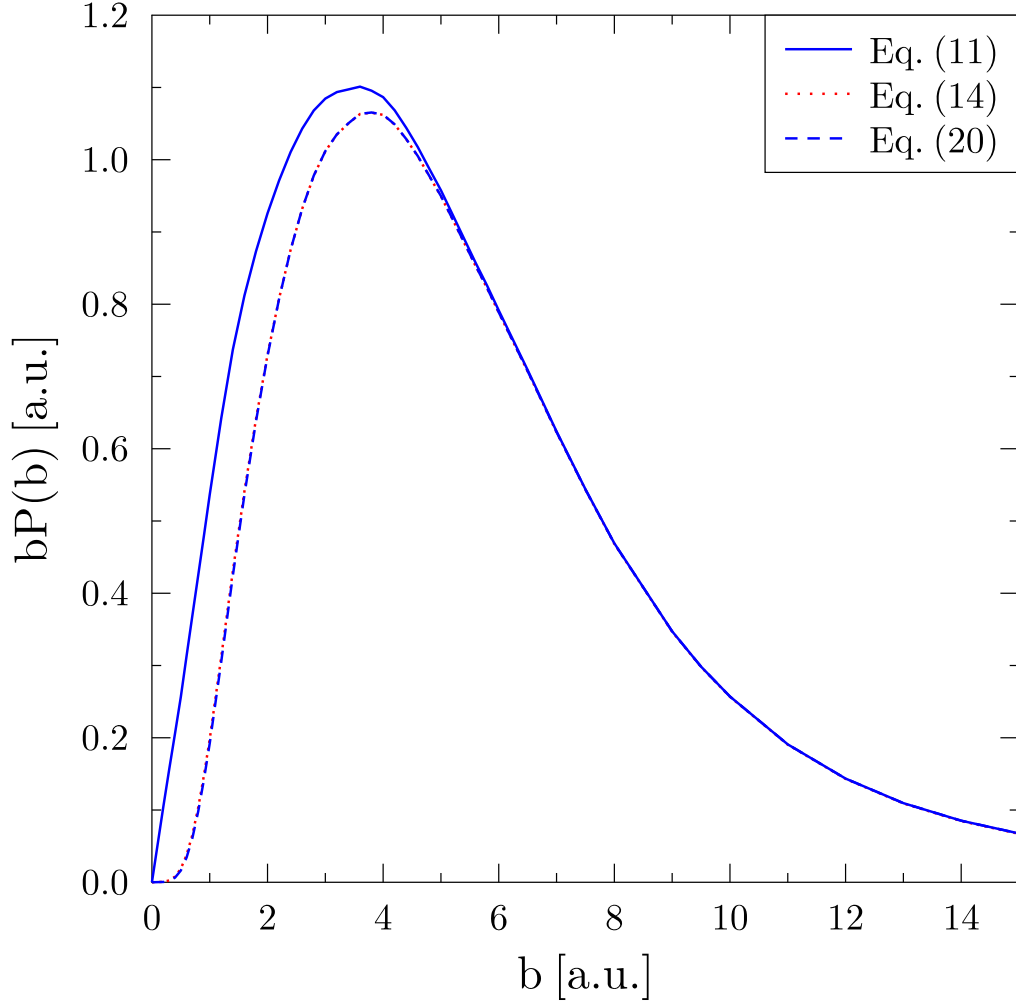


FIG. 2. (Color online) Impact-parameter-weighted probabilities for  $2s$  vacancy production [Eq. (14)], exclusive  $2s$  ionization [Eq. (20)], and single-particle  $2s$  ionization [Eq. (11)] for 1.5 MeV/amu  $O^{8+}$ -Li collisions. All curves shown are obtained from TC-BGM calculations. The curves displaying the probabilities (14) and (20) sit on top of each other.

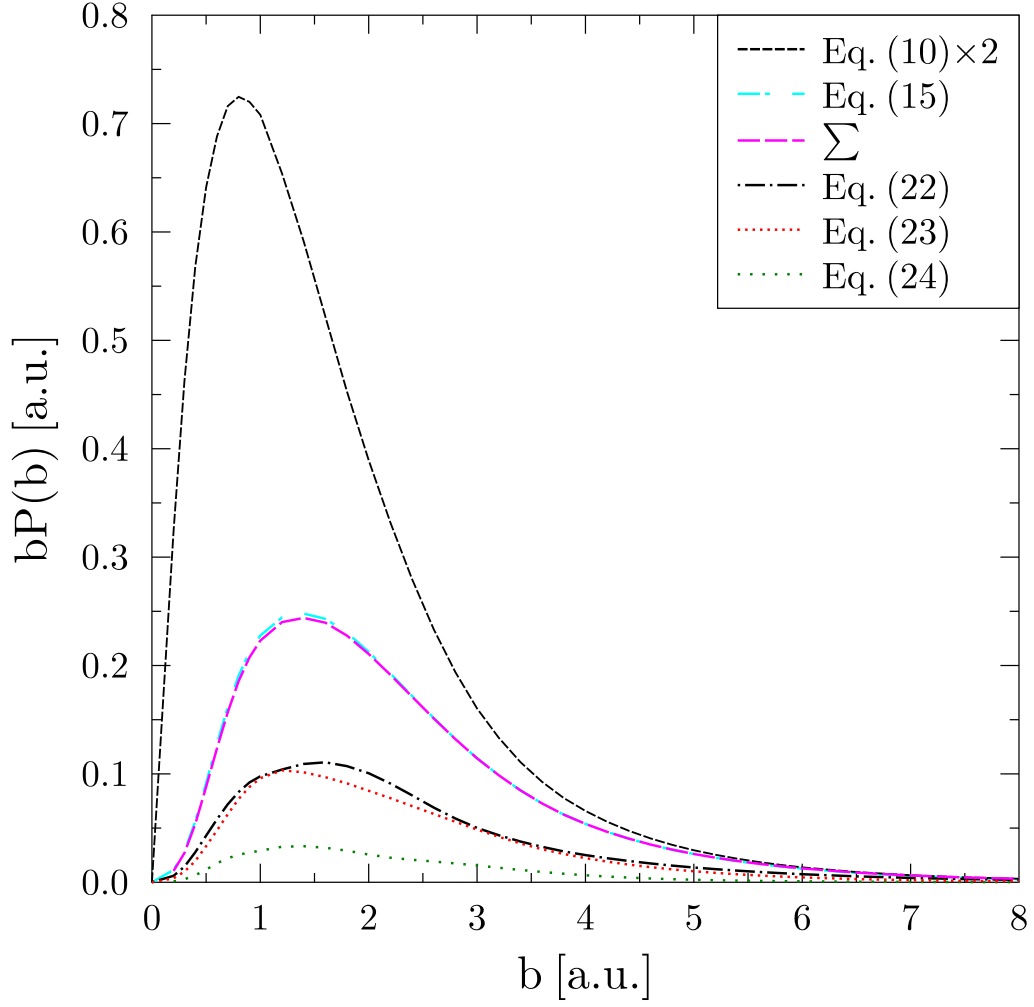


FIG. 3. (Color online) Impact-parameter-weighted probabilities for  $1s$  vacancy production [Eq. (15)], exclusive  $1s$  ionization [Eq. (22)],  $1s$  ionization with  $2s$  excitation [Eq. (23)],  $1s$  excitation with  $2s$  ionization [Eq. (24)], the sum of (22), (23) and (24) ( $\Sigma$ ), and single-particle  $1s$  ionization multiplied by two [Eq. (10) $\times 2$ ] for 1.5 MeV/amu  $O^{8+}$ -Li collisions. All curves shown are obtained from TC-BGM calculations.

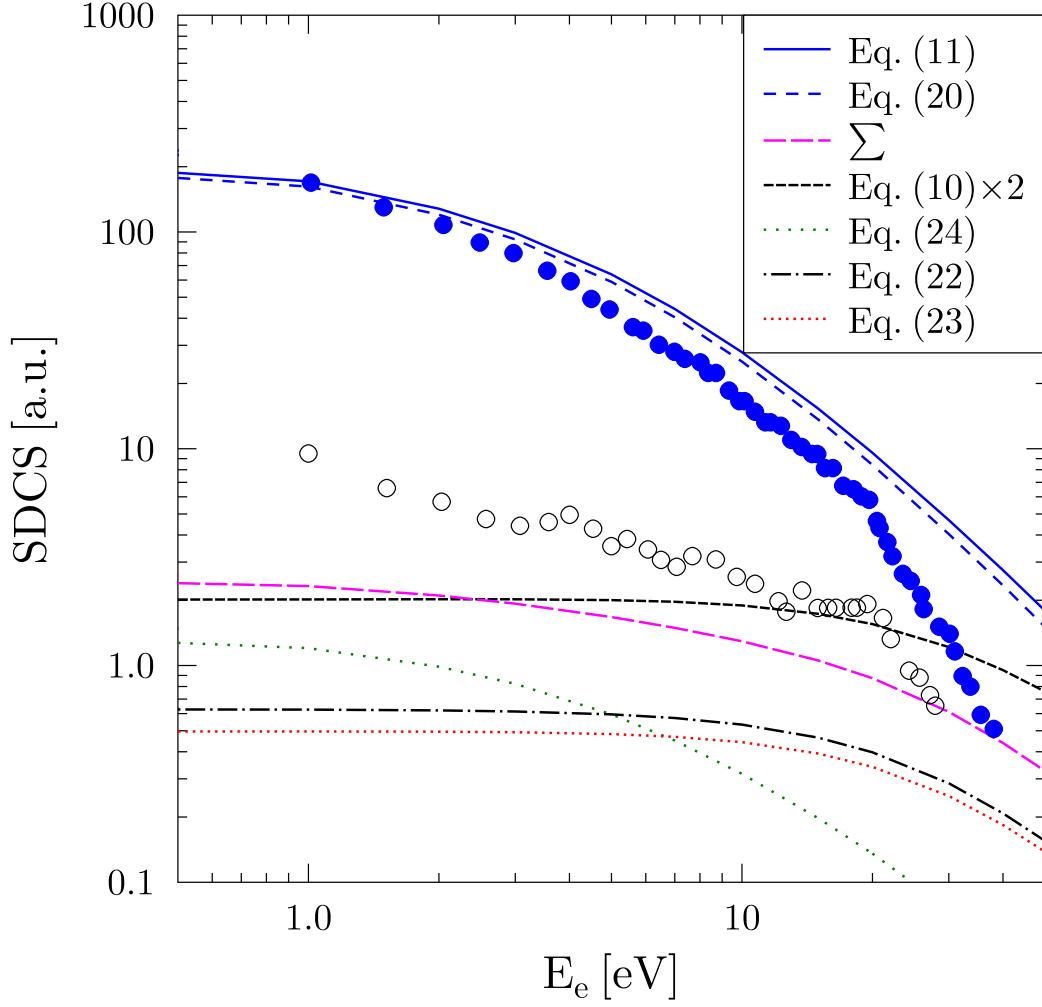


FIG. 4. (Color online) Single differential cross sections (SDCSs) for single-particle  $2s$  ionization [Eq. (11)], exclusive  $2s$  ionization [Eq. (20)], single-particle  $1s$  ionization multiplied by two [Eq. (10) $\times$ 2], exclusive  $1s$  ionization [Eq. (22)],  $1s$  ionization with  $2s$  excitation [Eq. (23)],  $1s$  excitation with  $2s$  ionization [Eq. (24)], and the sum of (22), (23) and (24) ( $\Sigma$ ) as functions of the electron energy for 1.5 MeV/amu  $O^{8+}$ -Li collisions. Experimental data: [8].

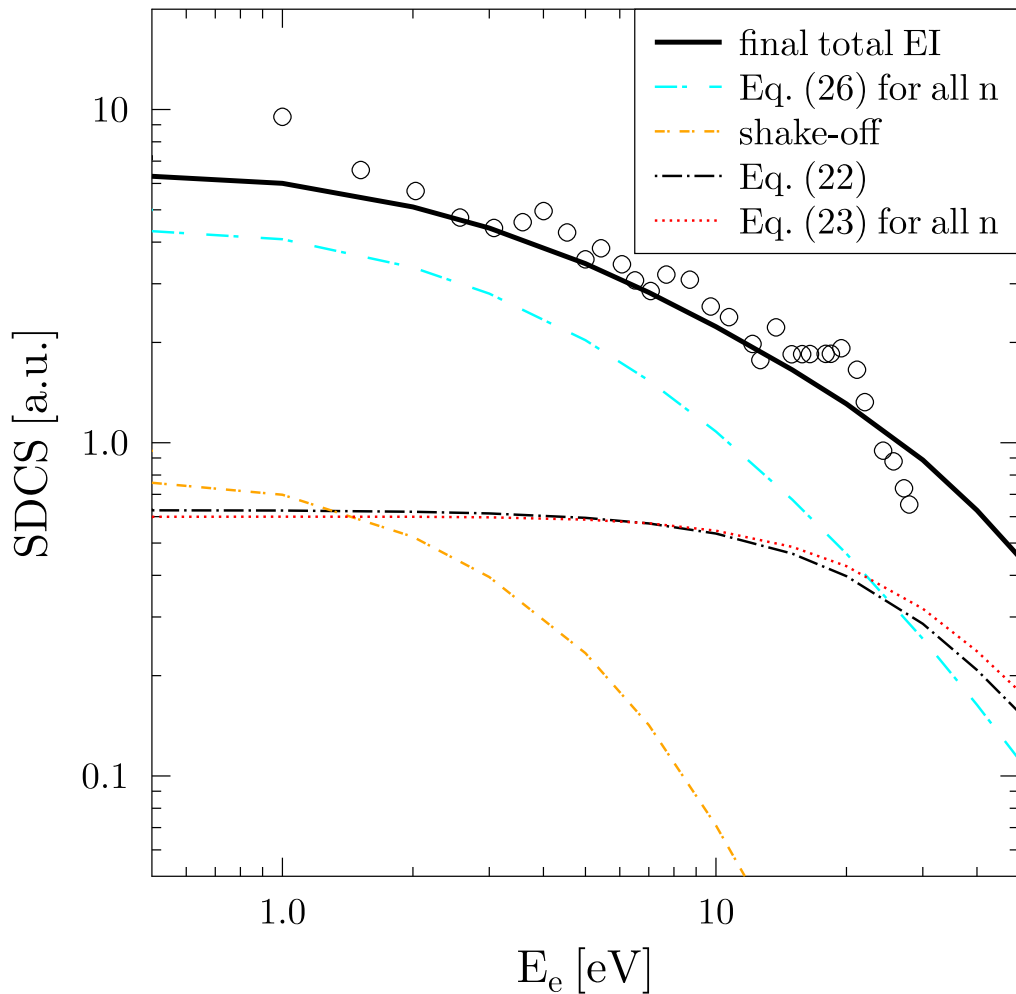


FIG. 5. (Color online) Single differential cross sections (SDCSs) for  $2s$  ionization with  $1s+$  excitation extrapolated to  $n \rightarrow \infty$  [Eq. (26) for all  $n$ ], the shake-off model as explained in the text, exclusive  $1s$  ionization [Eq. (22)], and  $1s$  ionization with  $2s$  excitation extrapolated to  $n \rightarrow \infty$  [Eq. (23) for all  $n$ ] as functions of the electron energy for 1.5 MeV/amu  $O^{8+}$ -Li collisions. The full thick curve dubbed 'final total EI' is obtained from adding the four other calculated SDCSs shown here and represents our final result for total EI. Experimental data: [8].

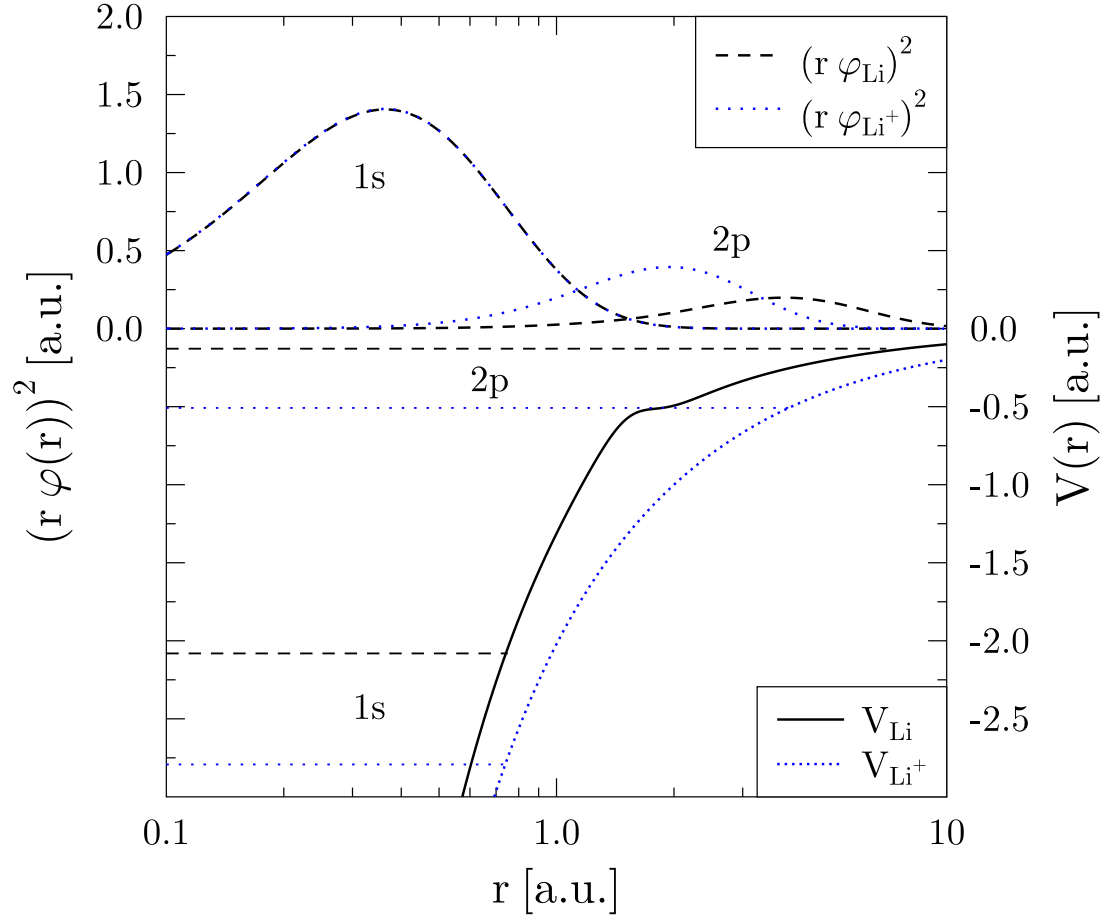


FIG. 6. (Color online) OPM potentials and  $1s$  and  $2p$  radial orbital densities for  $\text{Li}$  and  $\text{Li}^+$ . The  $\text{Li}(1s)$  and  $\text{Li}^+(1s)$  densities sit on top of each other. The horizontal lines indicate the binding energies of the  $1s$  and  $2p$  orbitals.